⌘ *Author's Choice*

THE JOURNAL OF BIOLOGICAL CHEMISTRY VOL. 287, NO. 35, pp. 29362–29372, August 24, 2012
© 2012 by The American Society for Biochemistry and Molecular Biology, Inc. Published in the U.S.A.

Cell Surface Expression of the Major Amyloid-β Peptide (Aβ)-degrading Enzyme, Neprilysin, Depends on Phosphorylation by Mitogen-activated Protein Kinase/Extracellular Signal-regulated Kinase Kinase (MEK) and Dephosphorylation by Protein Phosphatase 1a*[S]

Received for publication, January 6, 2012, and in revised form, June 27, 2012 Published, JBC Papers in Press, July 5, 2012, DOI 10.1074/jbc.M112.340372

Naomasa Kakiya[‡§1], **Takashi Saito**[‡1], **Per Nilsson**[‡], **Yukio Matsuba**[‡], **Satoshi Tsubuki**[‡], **Nobuyuki Takei**[§], **Hiroyuki Nawa**[§], **and Takaomi C. Saido**[‡2]

From the [‡]*Laboratory for Proteolytic Neuroscience, RIKEN Brain Science Institute, 2-1 Hirosawa, Wako-shi, Saitama 351-0198, Japan and the* [§]*Department of Molecular Neurobiology, Brain Research Institute, Niigata University, Niigata 951-8585, Japan*

Background: Neprilysin is a major Aβ-degrading enzyme, the expression of which is reduced in the AD brain.
Results: The phosphorylation status of the neprilysin intracellular domain regulates localization and cell surface activity.
Conclusion: Regulation of neprilysin through phosphorylation influences Aβ levels.
Significance: Our results indicate that neprilysin phosphorylation/dephosporylation could be one druggable target in the development of an AD-modifying treatment.

Neprilysin is one of the major amyloid-β peptide (Aβ)-degrading enzymes, the expression of which declines in the brain during aging. The decrease in neprilysin leads to a metabolic Aβ imbalance, which can induce the amyloidosis underlying Alzheimer disease. Pharmacological activation of neprilysin during aging therefore represents a potential strategy to prevent the development of Alzheimer disease. However, the regulatory mechanisms mediating neprilysin activity in the brain remain unclear. To address this issue, we screened for pharmacological regulators of neprilysin activity and found that the neurotrophic factors brain-derived neurotrophic factor, nerve growth factor, and neurotrophins 3 and 4 reduce cell surface neprilysin activity. This decrease was mediated by MEK/ERK signaling, which enhanced phosphorylation at serine 6 in the neprilysin intracellular domain (S6-NEP-ICD). Increased phosphorylation of S6-NEP-ICD in primary neurons reduced the levels of cell surface neprilysin and led to a subsequent increase in extracellular Aβ levels. Furthermore, a specific inhibitor of protein phosphatase-1a, tautomycetin, induced extensive phosphorylation of the S6-NEP-ICD, resulting in reduced cell surface neprilysin activity. In contrast, activation of protein phosphatase-1a increased cell surface neprilysin activity and lowered Aβ levels. Taken together, these results indicate that the phosphorylation status of S6-NEP-ICD influences the localization of neprilysin and affects extracellular Aβ levels. Therefore, maintaining S6-NEP-ICD in a dephosphorylated state, either by inhibition of protein kinases involved in its phosphorylation or by activation of phosphatases catalyzing its dephosphorylation, may represent a new approach to prevent reduction of cell surface neprilysin activity during aging and to maintain physiological levels of Aβ in the brain.

Impaired metabolism of amyloid β peptide (Aβ)[3] in the brain is likely to play a central role in the pathogenesis of Alzheimer disease (AD) (1). Genetically, causative genes in familial AD link mutations in amyloid precursor protein (APP) and presenilins to aberrant increased generation of Aβ42 and Aβ43, the 42- and 43-mer forms of Aβ, respectively. Aβ42 and Aβ43 have higher amyloidogenecity and neural toxicity than Aβ40 (1–4) and lead to the early onset of AD. However, Aβ amyloidosis in sporadic AD, which comprises over 90% of all AD cases, may be caused by a decline in Aβ degradation, Aβ clearance, or both (5). We previously identified neprilysin as a major physiological Aβ-degrading enzyme that regulates the steady-state levels of Aβ species in the brain (6, 7). Consistent with the increase in Aβ levels observed during aging and in AD, the expression levels of neprilysin in the brain decrease with age and in the early stages of AD (8–12). Genetic ablation of neprilysin not only markedly accelerates amyloid plaque formation but also leads to increased impairment of synaptic plasticity and memory formation in APP transgenic mice (13, 14). In contrast, elevation of neprilysin expression/activity promotes Aβ degradation and reduces the accumulation of both soluble and fibrillary Aβ in APP transgenic mice (15–17). Based on these observations, we previously searched for factors that could increase neprilysin activity pharmacologically, identifying somatostatin as a nepri-

* This study was supported by research grants from RIKEN Brain Science Institute; the Ministry of Education, Culture, Sports, Science, and Technology; and the Ministry of Health, Labor, and Welfare of Japan. This study was also supported by the Junior Research Associate Program of RIKEN.
⌘ *Author's Choice*—Final version full access.
[S] This article contains supplemental Figs. S1–S6.
[1] Both authors contributed equally to this work.
[2] To whom correspondence should be addressed. Tel.: 81-48-467-9715; Fax: 81-48-467-9716; E-mail: saido@brain.riken.jp.

[3] The abbreviations used are: Aβ, amyloid β peptide; AD, Alzheimer disease; APP, amyloid precursor protein; BDNF, brain-derived neurotrophic factor; CTF, C-terminal fragment of APP; ICD, intracellular domain; NEP, neprilysin; hNEP, human NEP; NT, neurotrophin; PP1 and PP2, protein phosphatase-1 and -2, respectively; SFV, Semliki Forest virus; MCA, methyl cumaryl amide.

lysin up-regulator, although the underlining mechanisms remain unclear (18).

In this study, we investigated the effect of the neurotrophic factors brain-derived neurotrophic factor (BDNF), nerve growth factor (NGF), and neurotrophins 3 and 4 (NT-3 and -4) and found that they cause a reduction in cell surface neprilysin activity through MAPK signaling. Moreover, our results reveal that cell surface neprilysin activity and localization are regulated by phosphorylation and dephosphorylation at the neprilysin intracellular domain, with a reduction in neprilysin activity leading to an increase in Aβ levels. We therefore speculate that possible drug targets involving neprilysin could include factors involved in the phosphorylation/dephosphorylation of this Aβ-lowering enzyme.

EXPERIMENTAL PROCEDURES

Materials—The reagents used in this study were purchased as follows: BDNF, NGF, NT-3, NT-4, cyclosporin A, and FK-506 (Sigma); U0126 (Enzo Life Sciences); fostriecin, okadic acid, and tautomycetin (Calbiochem); and recombinant human neprilysin (R&D Systems). The phospho-human neprilysin antibodies pS4-NEP, pS6-NEP, pT11-NEP, pT15-NEP, and pT25-NEP were obtained by immunizing rabbits with the following respective synthetic peptides containing phosphoserine (pS) or phosphothreonine (pT) residues: GKpSESQMC, GKSEpSQC, QMDIpTDINTC, TDINpTPKPKC, and KQRWpTPLEC (19, 20). The specificities of the purified phospho-antibodies were investigated by dot blot analysis (21) (see supplemental Fig. S3).

Cell Culture—Human SH-SY5Y neuroblastoma cells were obtained from the European Collection of Cell Cultures. Cells were cultured in 5% CO_2 at 37 °C, as previously described (22). The medium comprised a 1:1 mixture of minimum essential medium and Ham's F-12 medium (Nacalai Tesque), supplemented with 1 μM non-essential amino acids, 100 units/ml penicillin, 100 mg/ml streptomycin, and 15% fetal bovine serum (Invitrogen). Primary cortical/hippocampal neurons derived from wild-type or neprilysin-deficient mouse embryos were isolated as described previously (18). The neurons were plated at 5.0×10^4 cells/well in 96-well plates, 2.0×10^5 cells on glass coverslips (Hamanami) placed in 24-well plates, or 1.0×10^6 cells/well in 6-well plates. After 14 days *in vitro*, primary neurons were subjected to the various assays.

Mutagenesis and Transfection—S4A-, S6A-, T11A-, T15A- and T25A-human neprilysin mutants were generated using a KOD-Plus mutagenesis kit (Toyobo) according to the manufacturer's protocol. To introduce the mutations into human neprilysin cDNA previously cloned into pcDNA3.1 (23), the following primer sets were designed: S4A, 5′-GCAGAAAGTCAGATGGATATA-3′ and 5′-CTTGCCCATCACCTAGGCTGC-3′; S6A, 5′-GCTCAGATGGATATAACTGATATC-3′ and 5′-TTCTGACTTGCCCATCACCTAGG-3′; T11A, 5′-GCTGATATCAACACTCCAAAGC-3′ and 5′-TATATCCATCTGACTTTCTG-3′; T15A, 5′-GCTCCAAAGCCAAAGAAGAAACAGC-3′ and 5′-GTTGATATCAGTTATATCCATCTG-3′; and T25A, 5′-GGCTCCACTGGAGATCAGCCTCTCG-3′ and 5′-CATCGCTGTTTCTTCTTTGGCTTTG-3′ (underlined, original T, AG, A, A, and A, respectively). Constitutive active protein phosphatase-1a (PP1a)-T320A (24) was generated using the KOD-Plus mutagenesis kit, using the following primer set: 5′-GCCCCACCCCGCAATTCCGCCAAA-3′ and 5′-GATGGGTCGGCCTCCAGGGTTCAG-3′ (underlined, original A to G mutation). The mutant genes were transfected into SH-SY5Y cells using FuGENE transfection reagent (Roche Applied Science) according to the manufacturer's instructions. Cells were harvested with lysis buffer containing 0.1 M Tris-HCl, pH 7.5, EDTA-free complete protease inhibitor mixture (Roche Applied Science), 1% Triton X-100, 0.15 M NaCl, 1 mM Na_3VO_4, 1 mM NaF, and 1 μg/ml pepstatin A (Peptide Institute) 48–72 h after transfection.

Cell Surface and Whole-cell Neprilysin Activity—Activity staining of neprilysin using primary neurons was performed as described previously (18), with slight modifications. Because the endogenous neprilysin activity was too low in the primary neurons and SH-SY5Y cells, the cells were infected with Semliki Forest virus containing human neprilysin cDNA (SFV-hNEP), as previously described (25). Twenty-four h postinfection at day *in vitro* 14, neurotrophic factors or other reagents were added, and the cells were incubated for 24 h. They were then fixed with 1.5% paraformaldehyde in 50 mM phosphate buffer (pH 6.8) for 5 min at room temperature. The fixed neurons were incubated in substrate solution (0.25 mM glutaryl-Ala-Ala-Phe-methoxy-2-naphthylamide in 50 mM Tris-HCl, pH 7.4) at 37 °C for 2 h. Leucine aminopeptidase (Sigma), phosphoramidon (Peptide Institute), and nitrosalicylaldehyde (Sigma-Aldrich) were then added to the substrate solution at a final concentration of 50 μg/mg, 10 μM, and 0.6 mM, respectively, and incubated for 30 min at 37 °C. Quantification of the fluorescence signal arising from cell surface neprilysin activity was performed as described previously (18). Cell surface and whole-cell neprilysin activity of SH-SY5Y cells expressing mutant neprilysin were measured as described previously (26), with slight modifications (supplemental Fig. S5). Before the addition of neurotrophic factors, the cells were starved for 48 h to eliminate the effect of serum. After a 24-h treatment with neurotrophic factors, cells or lysates were incubated with substrate mixture (50 μM suc-Ala-Ala-Phe-MCA (Peptide Institute) and 10 nM benzyloxycarbonyl (Z)-Leu-Leu-Leucinal in 50 mM MES, pH 6.5, with or without 10 μM thiorphan (neprilysin-specific inhibitor)) at 37 °C for 30 min. Following this, 0.1 mg/ml leucine aminopeptidase (Sigma) and 0.1 mM phosphoramidon were added, and the reaction mixture was incubated at 37 °C for a further 30 min. 7-Amino-4-methylcoumarin fluorescence was measured at excitation and emission wavelengths of 380 and 460 nm, respectively. After measurement, cells were collected and subjected to Western blot analysis to evaluate neprilysin levels.

Cell Surface Biotinylation—The cell membrane of cortical/hippocampal neurons or SH-SY5Y cells was biotinylated with sulfo-NHS-SS-biotin (Pierce), according to the manufacturer's instructions. The samples were subsequently subjected to immunocytochemical study or pull-down assay. Biotinylated cell surface proteins were pulled down using Biotin-Capture beads (Adar Biotech).

Immunocytochemical Study—To visualize and quantify neprilysin localization in cortical/hippocampal neurons, the cells were infected with SFV-hNEP, and the cell surface was

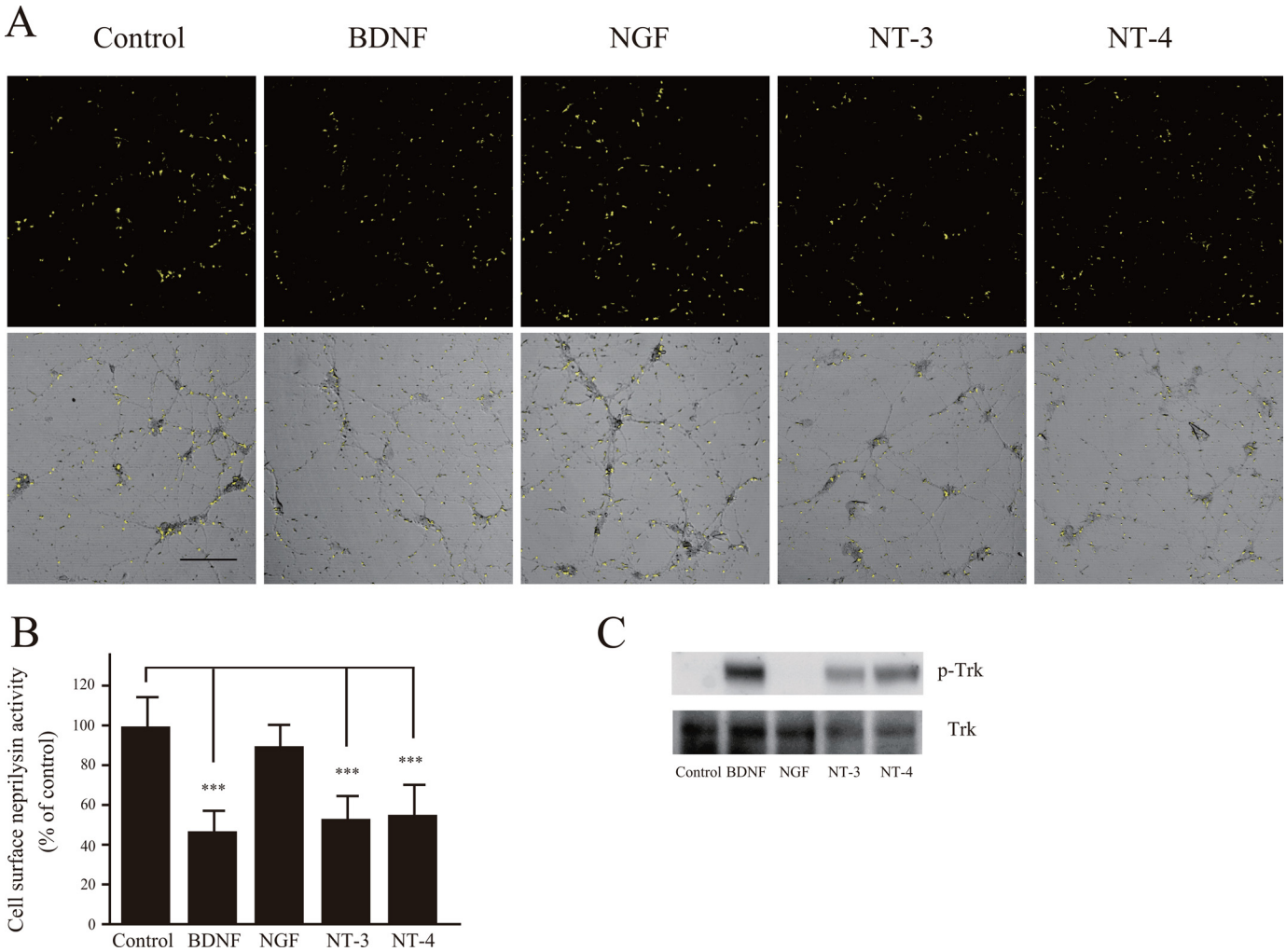

FIGURE 1. **Neurotrophic factors reduce cell surface neprilysin activity in primary cortical/hippocampal neurons.** *A*, primary cortical/hippocampal neurons infected with SFV-hNEP were incubated with BDNF (100 ng/ml), NGF (100 ng/ml), NT-3 (100 ng/ml), or NT-4 (100 ng/ml) for 24 h, after which they were subjected to the neprilysin activity-staining assay. The *top panels* show fluorescence images representing neprilysin activity, and the *bottom panels* show phase-contrast images merged with the *top panels*. *Scale bar*, 100 μm. *B*, quantification of the fluorescence signal areas, indicated as average ± S.D. (*error bars*) ($n = 5$). ***, $p < 0.01$ compared with control. *C*, primary neurons were incubated with BDNF (100 ng/ml), NGF (100 ng/ml), NT-3 (100 ng/ml), or NT-4 (100 ng/ml) for 30 min and then subjected to Western blot analysis to measure the phosphorylation level of the neurotrophic factor receptor, Trk, using antibodies against Trk receptor (*bottom*) and phosphorylated Trk (*p-Trk*; *top*). At least three independent experiments were repeated.

labeled with biotin. The cells grown on coverslips were fixed with 100% ice-cold MeOH for 10 min at −20 °C and permeabilized in 100% ice-cold acetone for 1 min at −20 °C. After blocking with blocking buffer (phosphate-buffered saline containing 5% skim milk, 5% goat serum, and 0.05% Tween 20) for 30 min at room temperature, the samples were incubated with primary anti-human neprilysin antibody (1:100, Novocastra) in blocking buffer for 1 h at room temperature, followed by secondary anti-mouse Alexa 488 (1:500, Invitrogen) and Streptavidin-Alexa 546 (1:500; Molecular Probes) antibody for 30 min at room temperature. The fluorescence signals observed by confocal microscopy were quantified by counting signal dots, as described previously (27).

Immunoprecipitation and Western Blot Analysis—Cell lysates from primary cortical/hippocampal neurons infected with SFV-hNEP were immunoprecipitated with mouse monoclonal anti-human neprilysin (SN5c/L4–1A1, Ancell). Samples were subjected to Western blot analysis using the following antibodies: phospho-human neprilysin antibodies (supplemental Fig. S3), anti-human neprilysin (56C6, Novocastra), anti-mouse neprilysin (421126, Techne), antibodies recognizing the N-terminal region of APP (22C11, Chemicon) or the C-terminal region of APP (A8717, Sigma), anti-PP1A (Thr(P)-320) (EP1512Y, Novus), anti-PP1α (Santa Cruz Biotechnology, Inc., Santa Cruz, CA), anti-phospho-TrkA (Tyr-490, Cell Signaling), anti-Trk (B-3, Cell Signaling), anti-phospho-Erk1/2 (Thr-202/Tyr-204, Cell Signaling), anti-Erk1/2 (Cell Signaling), anti-Myc (9B11, Cell Signaling), anti-G3PDH/GAPDH (Trevigen), or anti-β-actin (AC-15, Sigma-Aldrich).

Aβ ELISA—Conditioned medium from control cortical/hippocampal neurons or those treated with neurotrophic factors for 24 h and from SH-SY5Y cells transiently expressing wild-type neprilysin (WT-NEP), S6A-NEP, WT-PP1a, and T320A-PP1a were collected, and guanidine HCl was added as described previously (4). In order to achieve a measurable level of Aβ40 in the conditioned medium from SH-SY5Y cells transfected with WT-NEP or S6A-NEP, 200 pM Aβ40 peptide was added to the samples. Samples were analyzed using Aβ-ELISA kits (Wako)

to quantify Aβ40 and Aβ42, according to the manufacturer's instructions.

Statistical Analysis—All of the values are presented as mean ± S.D. Statistical analysis was performed by one-way analysis of variance with Scheffe's F test.

RESULTS

Neurotrophic Factors Reduce Neprilysin Activity via MAPK Signal Transduction—Membrane-bound neprilysin located on the cell surface participates in extracellular Aβ degradation and therefore plays a key role in Aβ metabolism. We have previously established an activity-staining method for primary neurons that visualizes neprilysin activity on the cell surface (18, 25). In a search for regulators of neprilysin activity, we identified somatostatin, which was found to exert an up-regulatory effect (18). To further unravel the mechanisms regulating neprilysin activity, we screened the neurotrophic factors BDNF, NGF, NT-3, and NT-4 using our activity-staining technique on primary cortical/hippocampal neurons. Representative images of such activity-staining experiments are shown in Fig. 1. Interestingly, BDNF, NT-3, and NT-4 all significantly reduced neprilysin activity, whereas NGF had no effect. However, given that cortical/hippocampal neurons do not express the TrkA receptor subtype to which NGF binds (28), we also examined the effect of NGF on primary neurons derived from the striatum. Indeed, exposing striatal primary neurons to NGF induced a reduction in neprilysin activity (supplemental Fig. S1, *A* and *B*). To confirm activation of the signal transduction pathway leading to a reduction in neprilysin, phosphorylation of Tyr-490 in Trk was measured (29). Upon exposure of the primary neurons to BDNF, NGF, NT-3, or NT-4, phosphorylation of Trk significantly increased (Fig. 1*C* and supplemental Fig. S1*C*), indicating that the Trk receptors were activated.

To further elucidate the Trk receptor-induced transduction pathway, we next investigated the effects of U0126, LY294002, and calphostin C, inhibitors of MAPK/ERK kinase 1/2 (MEK1/2), phosphatidylinositol-3 kinase, and protein kinase C, respectively, on cell surface neprilysin activity (30). First, we co-treated neurons with BDNF, NGF, NT-3, or NT-4 together with U0126 and found that U0126 completely inhibited the reduction in cell surface neprilysin activity induced by the neurotrophic factors (Fig. 2), indicating the involvement of MAPK/ERK kinase in the signaling pathway. We then focused on NT-3 because it binds to all Trk receptor subtypes (*i.e.* TrkA, -B, and -C) (28). Simultaneous treatment of neurons with NT-3 and calphostin C did not inhibit the reduction in neprilysin activity. Finally, LY294002 treatment alone produced a decrease in cell surface neprilysin activity. However, because LY294002 in combination with NT-3 did not inhibit the NT-3-induced reduction in neprilysin activity (supplemental Fig. S1*D*), it is possible that the effect of LY294002 involves a pathway independent of the Trk signaling pathway. Thus, together these results indicate that neurotrophic factors reduce cell surface neprilysin activity in neurons via the MEK/ERK signaling pathway.

Although binding of neurotrophic factors to Trk receptors is known to activate the MAPK pathway within 30 min (31) (Fig. 1*C*), the levels of cell surface neprilysin activity remained unaltered 30 min after the addition of the neurotrophic factors (supplemental Fig. S1*E*). Rather, the effect became clearly visible 24 h poststimulation (Fig. 1, *A* and *B*). Taken together, these findings indicate that neurotrophic factors reduce cell surface neprilysin activity by binding to neuronal Trk receptors and subsequent activation of the MAPK pathway. The mechanistic explanation behind the delayed effect is currently not known but could include changes in, for example, gene expression of additionally required factors.

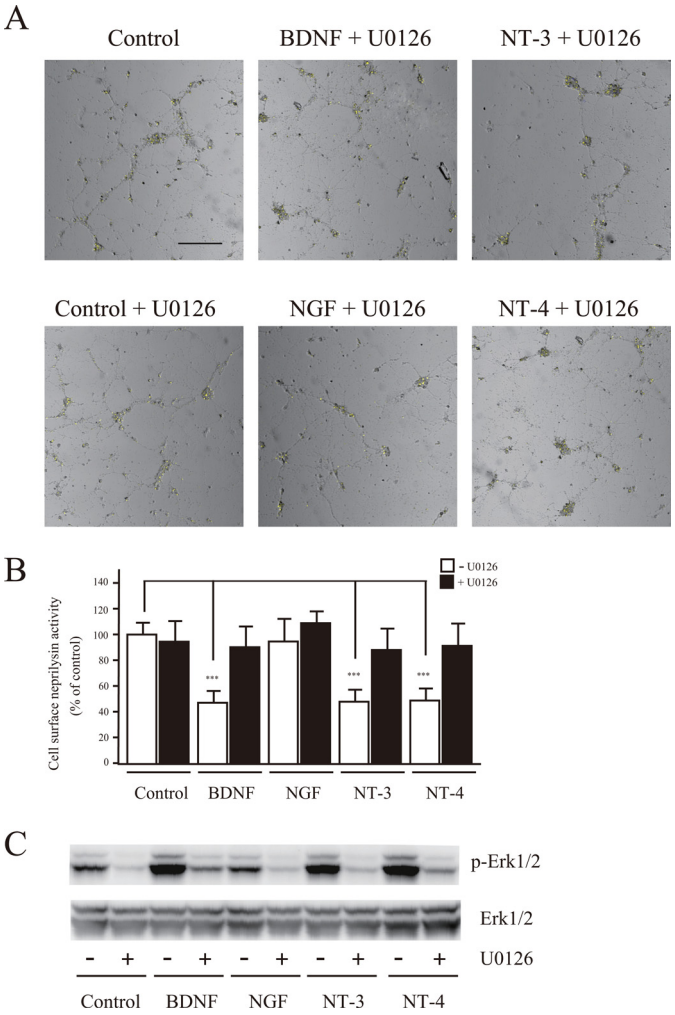

FIGURE 2. **Reduction of neprilysin activity by neurotrophic factors involves the MEK1/2 signaling pathway.** *A*, primary cortical/hippocampal neurons infected with SFV-hNEP were co-incubated with BDNF (100 ng/ml), NGF (100 ng/ml), NT-3 (100 ng/ml), or NT-4 (100 ng/ml) and the MEK1/2 inhibitor U0126 (1 μM), for 24 h, after which they were subjected to the neprilysin activity-staining assay. Representative fluorescence images merged with phase-contrast images are shown. *Scale bar*, 100 μm. *B*, quantification of the fluorescence signal derived from neprilysin activity was performed, and the results are presented as average ± S.D. (*error bars*) ($n = 5$). ***, $p < 0.01$ compared with control. *C*, primary neurons were incubated with or without U0126, as indicated, and neurotrophic factors for 30 min and were then subjected to Western blot analysis to measure the phosphorylation levels of MAPK using antibodies against Erk1/2 (*bottom*) and phosphorylated Erk1/2 (*p-Erk1/2*; *top*). At least three independent experiments were repeated.

Effect of NT-3 on Aβ Levels—A reduction in neprilysin induced by neurotrophic factors would presumably lead to increased Aβ levels. We therefore measured Aβ levels in conditioned medium from primary neurons infected with SFV-hNEP, using the same conditions as for the activity assay. How-

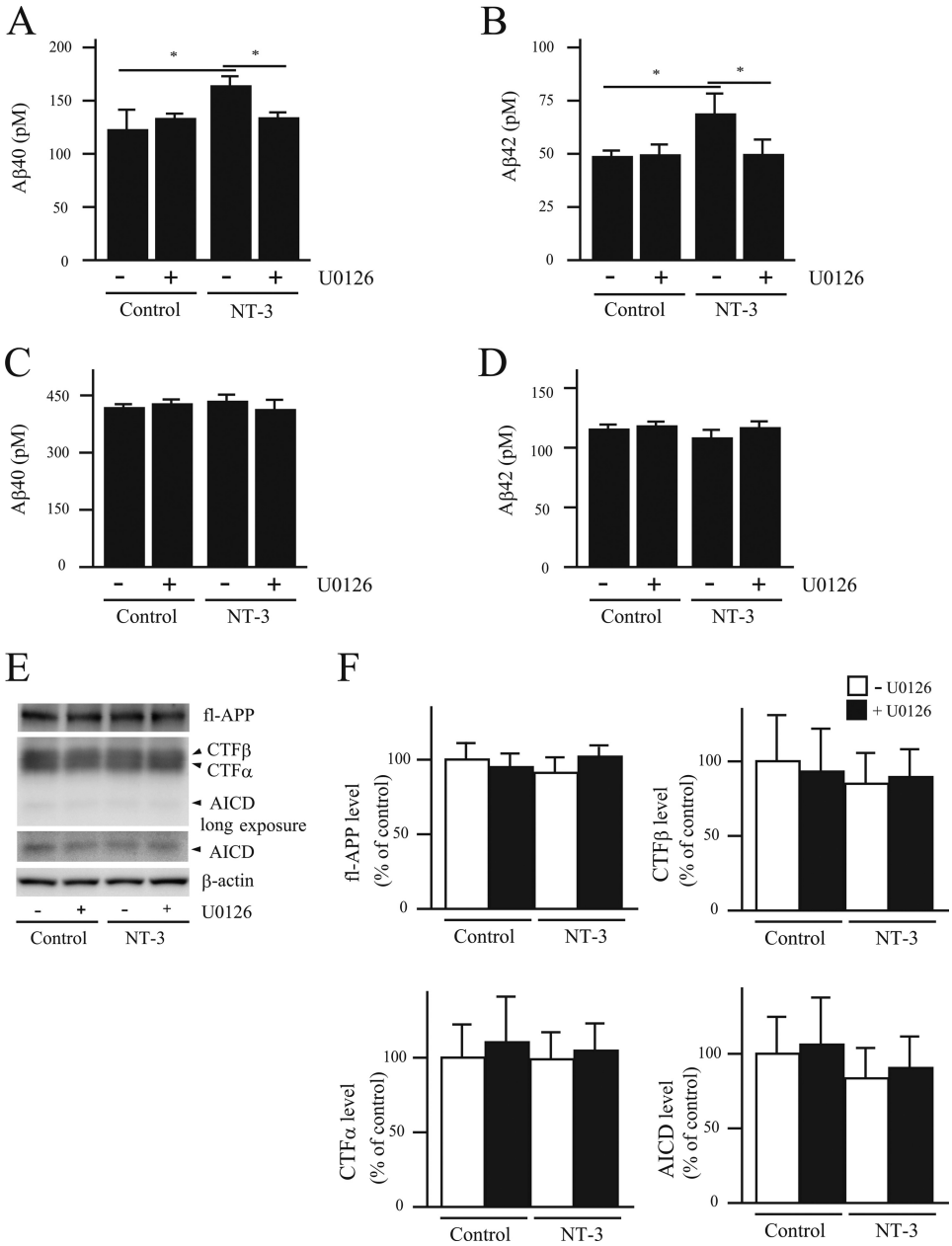

FIGURE 3. **NT-3 induces increased Aβ levels via the MEK/ERK pathway.** *A–D*, the culture medium of primary neurons derived from wild-type (*A* and *B*) or NEP-deficient mouse embryos (*C* and *D*) was collected 24 h after NT-3 (100 ng/ml) treatment with or without U0126 (1 μM) and then subjected to Aβ ELISA. Aβ40 (*A* and *C*) and Aβ42 (*B* and *D*) levels were measured using an Aβ-ELISA kit. Each *column* with *error bar* represents the mean ± S.D. ($n = 4$). *, $p < 0.05$ compared with control and co-treatment. *E* and *F*, the effect of neurotrophic factors on Aβ generation was investigated by measuring the levels of full-length APP (*fl-APP*), CTFα, CTFβ, APP intracellular domain (*AICD*), and β-actin in the primary neurons by Western blot. Intensities of each band were quantified by densitometric analysis, and data represent the mean ± S.D. ($n = 5$).

ever, due to the high viral expression of neprilysin, the Aβ levels were too low to be detected. Therefore, we instead measured the conditioned medium from non-infected primary cortical/hippocampal neurons. NT-3 treatment significantly increased the steady-state levels of Aβ40 and Aβ42, an effect that was abolished by the addition of U0126 (Fig. 3, *A* and *B*). Importantly, treating primary neurons derived from neprilysin-deficient mice with NT-3 did not affect Aβ levels, showing that the increased Aβ levels generated from wild-type neurons are due specifically to a decrease in neprilysin activity (Fig. 3, *C* and *D*). Furthermore, full-length APP levels and the levels of the C-terminal fragments of APP, CTFα, CTFβ, and APP intracellular domain, which are produced by α-, β- and γ-secretase, respectively, and used as an index of secretase activity (32) were not altered by NT-3 treatment (Fig. 3, *E* and *F*). These results together suggest that the increased steady-state levels of Aβ upon NT-3 treatment are due specifically to a decrease in cell surface neprilysin activity rather than increased Aβ generation in the neurons. Finally, to ascertain that the increased Aβ levels observed upon NT-3 treatment were specifically due to decreased levels of cell surface neprilysin, the levels of the Aβ-degrading enzymes endothelin-converting enzyme-1 (33) and insulin-degrading enzyme (34) were investigated. Neither the levels of endothelin-converting enzyme-1 and insulin-

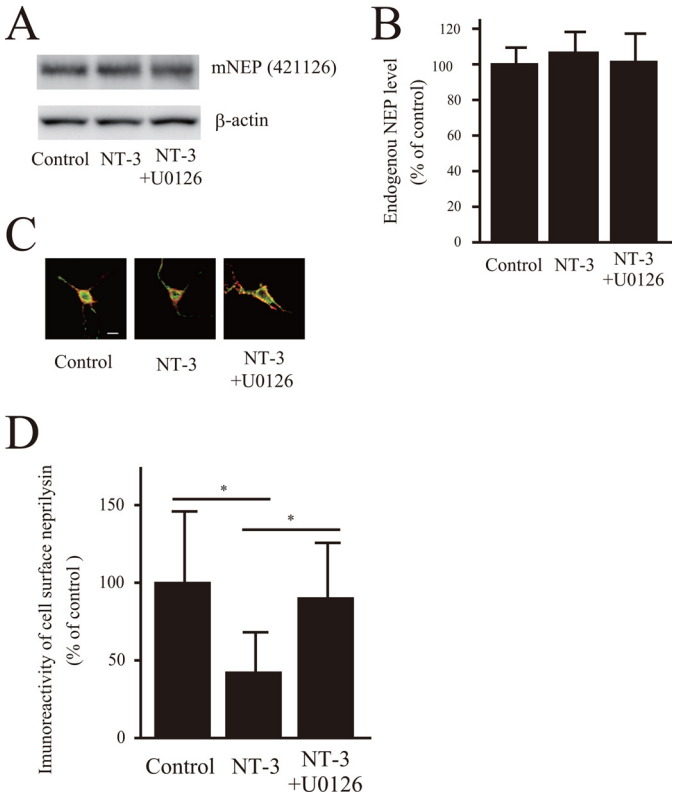

FIGURE 4. **NT-3 regulates neprilysin localization via the MEK/ERK pathway.** *A* and *B*, the effect of NT-3 on expression levels of neprilysin in primary neurons was analyzed by Western blot analysis. The experiments were repeated four times, and the results are presented as mean values ± S.D. (*error bars*). *C* and *D*, double staining for neprilysin and biotinylated proteins located on the cell surface. Primary cortical neurons infected with SFV-hNEP were treated with NT-3 (100 ng/ml) for 24 h. The cell surface proteins were subsequently cross-linked with biotin, after which the cells were double-stained with neprilysin antibody (56C6; *green*) and Alexa 546-conjugated streptavidin (*red*). The images of the *green* and the *red* signals were merged, *yellow* representing cell surface neprilysin. *Scale bar*, 50 μm. The ratio of cell surface neprilysin levels was quantified by image analysis. Data represent the mean ± S.D. ($n = 15$). *, $p < 0.05$ compared with control and co-treatment.

degrading enzyme nor the activity of insulin-degrading enzyme were affected by NT-3 treatment (supplemental Fig. S2, *A* and *B*). These data, together with the lack of changes in Aβ levels secreted from primary neurons prepared from neprilysin knock-out mice and stimulated with neurotrophic factors, lead us to conclude that decreased levels in cell surface neprilysin expression are responsible for the increased Aβ levels.

NT-3 Alters Neprilysin Localization in Neurons—To address whether the NT-3-induced reduction in neprilysin was due to changes in neprilysin expression, we quantified neprilysin levels in whole-cell lysates before and after NT-3 treatment. Western blot data clearly showed that neprilysin expression levels were not altered after NT-3 treatment (Fig. 4, *A* and *B*). Therefore, we next performed immunocytochemical experiments to visualize neprilysin in the neurons. Proteins located on the cell surface were biotinylated, after which the cells were immunocytochemically stained with avidin and anti-neprilysin antibody and analyzed as described under "Experimental Procedures." Quantitative image analysis revealed that the level of neprilysin located on the cell surface was significantly reduced upon NT-3 treatment (Fig. 4, *C* and *D*). Importantly, the addition of U0126 restored this level to normal. Taken together, these results indicate that neurotrophic factors modulate neprilysin localization through MEK/ERK signaling, without affecting neprilysin expression levels, leading to a decrease in cell surface neprilysin activity and ultimately resulting in increased extracellular Aβ levels.

MEK/ERK Signaling Modulates the Phosphorylation State of the Neprilysin Intracellular Domain—The localization of plasma membrane-associated proteins is often regulated by phosphorylation/dephosphorylation at the intracellular domain (ICD) of the protein (35). Because neprilysin is a type II membrane protein, its N-terminal side is located in the cytoplasmic lumen. As shown in Fig. 5*A*, there are five potential amino acid residues in human neprilysin and four in mouse neprilysin ICD (NEP-ICD) that could possibly be phosphorylated. In order to accurately determine the phosphorylation state of the NEP-ICD, we first generated the phosphoserine- and phosphothreonine-specific antibodies pS4-NEP, pS6-NEP, pT11-NEP, pT15-NEP, and pT25-NEP, which specifically recognize individual phosphorylated threonine and serine residues in the NEP-ICD, respectively. The specificities of these antibodies are summarized in supplemental Fig. S3. We then probed cell extracts of primary neurons using this battery of phospho-antibodies. Although the endogenous expression level of neprilysin is low, we were able to detect phosphorylation of Ser-4, Ser-6, and Thr-11 in neprilysin (Fig. 5). We were not able to detect pT25-NEP due to limited affinity of the antibody. Interestingly, upon exposing primary neurons to NT-3, phosphorylation of Ser-6 increases significantly. Simultaneously treating the cells with NT-3 and U0126 inhibited the increase in phosphorylation of Ser-6 induced by NT-3, implying that the MAPK pathway is involved in the regulation of NEP-ICD phosphorylation (Fig. 5, *B* and *C*).

Because the endogenous neprilysin level in primary neurons is low and our aim was to study the regulatory mechanism of human neprilysin, we continued our studies using SFV-hNEP-infected primary neurons. After infection, we investigated the phosphorylation state of NEP-ICD. Consistent with phosphorylation of Ser-6 of endogenous neprilysin, we detected that overexpressed human neprilysin also was phosphorylated at Ser-6 upon treatment with NT-3. Further, the effect was inhibited by the addition of U0126. In addition, a trend toward increased Ser-4 phosphorylation was detected together with increased phosphorylation of Thr-15 (Fig. 5, *B* and *C*). Subsequently, we examined whether neprilysin localized to the cell surface exhibits different phosphorylation statuses compared with intracellularly located neprilysin. Biotinylated proteins located on the cell surface of SFV-hNEP-infected primary neurons were first pulled down from cell lysates using Biotin-Capture beads, after which intracellular neprilysin was collected using a neprilysin-specific antibody. Although all potential phosphorylation sites in the NEP-ICD of intracellularly located neprilysin were phosphorylated, no phosphorylation of Ser-6 or Thr-25 could be detected in neprilysin present in the cell surface fraction (Fig. 5*D*). These results together indicated that treating the cells with NT-3 for 24 h resulted in extensive phosphorylation of Ser-6 and Thr-15 of cell surface-located neprilysin. Although activation of Trk receptors was detected 30 min

after the addition of NT-3 to the cells, there was no difference in the phosphorylation state of NEP-ICD after a 30-min treatment by NT-3 (data not shown). The reasons behind the delayed effect are currently not known. Furthermore, the increase in phosphorylation of Ser-4, Ser-6, and Thr-15 induced by NT-3 was inhibited by the addition of U0126, indicating the involvement of MAPK in the signaling pathway (Fig. 5, *B* and *C*). Together, the data indicate that phosphorylation of Ser-6 is involved in the regulation of cell surface neprilysin.

To further clarify the role of human NEP-ICD phosphorylation in neprilysin activity, we generated five mutants in which

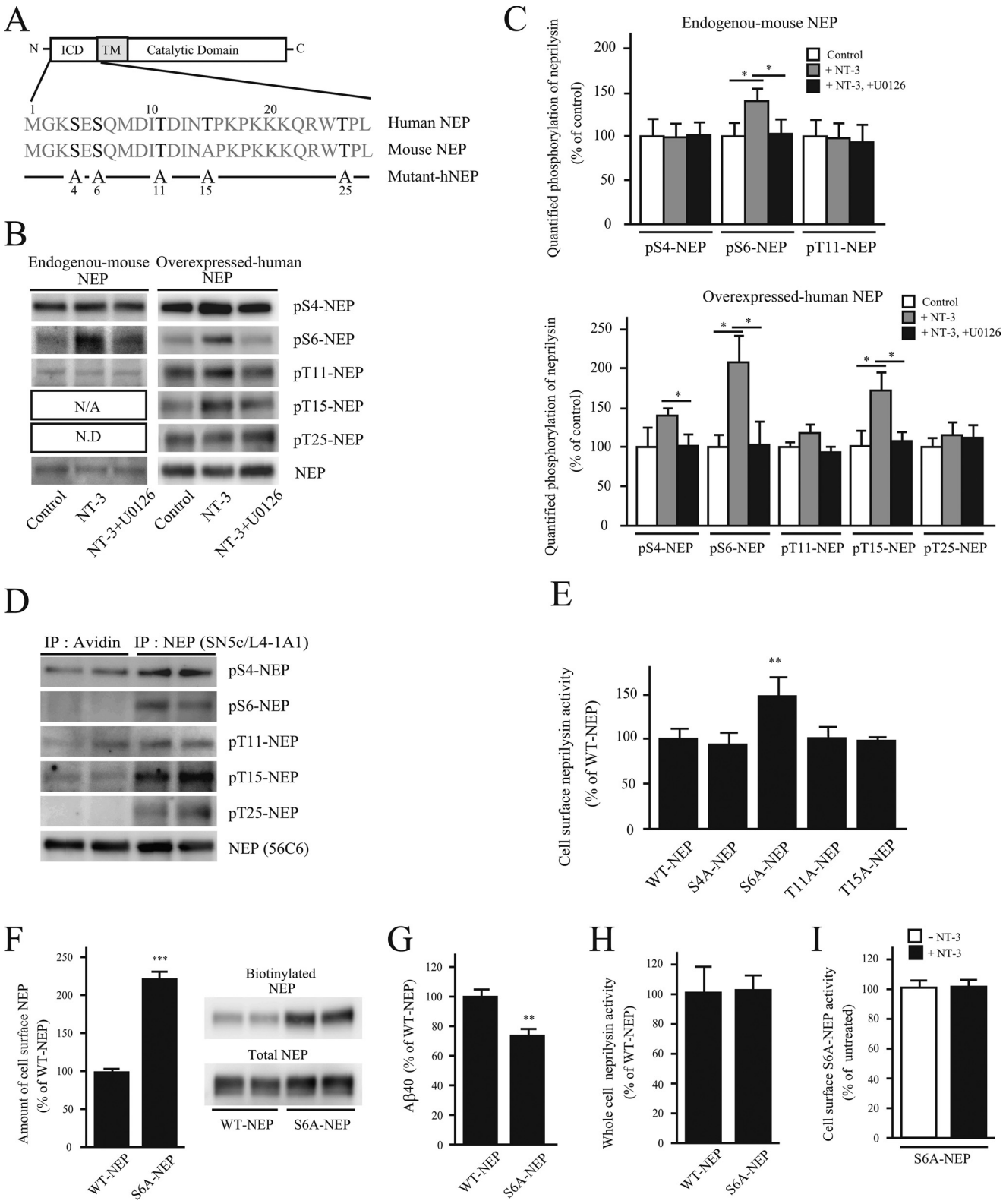

the putative serines/threonines in the NEP-ICD were substituted with alanines (*i.e.* S4A-, S6A-, T11A-, T15A-, and T25A-NEP, respectively) (Fig. 5*A*). The selection of a cell line for the mutational analysis was based on two criteria: 1) it should be a human neuronal cell line, and 2) it should express endogenous neprilysin to assure that the regulatory mechanisms of neprilysin are preserved. The endogenous expression of neprilysin in SH-SY5Y was confirmed with Western blot (Fig. S5*A*). Thus, the mutants were introduced into SH-SY5Y cells, and cell surface neprilysin activity was measured and normalized to expression levels. Interestingly, S6A-NEP transfectants showed significantly higher cell surface activity than S4A-, T11A-, T15A-, and WT-NEP transfectants (Fig. 5*E* and supplemental Fig. S4). The effect of T25A-NEP on neprilysin activity could not be evaluated due to its low expression (supplemental Fig. S5). We also subsequently measured the amount of cell surface-located S6A-NEP and found it to be significantly higher than that of WT-NEP (Fig. 5*F*). In accordance with the increased cell surface activity of S6A-NEP, the extracellular Aβ40 level in conditioned medium from S6A-NEP transfectants was significantly lower than that for WT-NEP transfectants (Fig. 5*G*). Furthermore, the total neprilysin activity, normalized to expression levels, in whole-cell lysates from WT-NEP and S6A-NEP transfectants were similar (Fig. 5*H*). This indicates that the increase in cell surface neprilysin activity observed in the case of S6A-NEP was not due to an allosteric effect induced by the mutation. Last, the cell surface neprilysin activity of S6A-NEP transfectants was not affected by NT-3 treatment (Fig. 5*I*). Taking all of the data together, we conclude that phosphorylation of Ser-6 of the NEP-ICD regulates neprilysin localization and thereby neprilysin cell surface activity via MEK/ERK signaling.

PP1a Facilitates Cell Surface Neprilysin Activity—Given that phosphorylation of Ser-6 in the NEP-ICD influences neprilysin cell surface localization, we next evaluated the effects of different phosphatase activities on neprilysin localization and activity. Primary cortical/hippocampal neurons infected with SFV-hNEP were treated with the following specific inhibitors for serine/threonine phosphatases: tautomycetin (PP1a inhibitor), fostriecin and okadaic acid (PP2A inhibitors), and cyclosporin A and FK-506 (PP2B/calcineurin inhibitors). Interestingly, treatment with the PP1a inhibitor tautomycetin resulted in significantly increased phosphorylation of the S6-NEP-ICD (Fig. 6, *A* and *B*) and decreased cell surface neprilysin activity (Fig. 6*C*). In addition to S6-NEP-ICD, phosphorylation of S4- and T11-NEP-ICDs was also increased by tautomycetin. However, phosphorylation of Ser-4 and Thr-11 did not influence cell surface neprilysin activity (Fig. 5 and supplemental Fig. S6).

The increased phosphorylation of Ser-6 upon PP1a inhibition suggests an association of neprilysin and PP1a. Previously, PTEN (phosphatase and tensin homolog deleted from chromosome 10), which is a tumor suppressor and acts as a tyrosine phosphatase, has been shown to be associated with the NEP-ICD (36). Interestingly, an amino acid sequence found in the NEP-ICD, KKKQRW, is similar to a PP1a-interacting sequence (37, 38). This finding prompted us to investigate a possible interaction between neprilysin and PP1a. We therefore performed immunoprecipitation experiments using SH-SY5Y cell lysates from mock and WT-NEP transfectants. The results revealed that neprilysin co-immunoprecipitates not only with PTEN but also with PP1a, indicating that the proteins are directly or indirectly associated (Fig. 6*D*).

To confirm the role of PP1a in neprilysin dephosphorylation and localization, and because PP1a is activated by dephosphorylation at the threonine 320 residue, we prepared a constitutive active mutant PP1a, which harbors a T320A mutation (Fig. 6*E*) (24). Expression of both WT-PP1a and T320A-PP1a in SFV-hNEP-infected SH-SY5Y cells induced an increase in cell surface neprilysin activity compared with mock transfectants. Moreover, constitutive active T320A-PP1a transfectants exhibited significantly higher cell surface neprilysin activity compared with WT-PP1a transfectants (Fig. 6*F*).

In addition, extracellular Aβ levels were significantly reduced by both WT-PP1a and T320A-PP1a expression (Fig. 6*G*). Taken together, these results suggest that activation of PP1a increases cell surface neprilysin activity/localization is due, at least partly, to dephosphorylation of Ser-6 in the NEP-ICD.

DISCUSSION

Pharmacological maintenance or enhancement of the major Aβ-degrading enzyme neprilysin during aging could offer a possible treatment for the prevention of AD. Accumulating evi-

FIGURE 5. **Dephosphorylation of the neprilysin intracellular domain localizes neprilysin to the cell surface.** *A*, scheme of human and mouse neprilysin domain structure and the N-terminal amino acid sequences corresponding to the neprilysin intracellular domain. *ICD* and *TM*, intracellular domain and transmembrane domain of neprilysin, respectively. Potential phosphorylation sites are indicated in *boldface type*. *Below*, the substituted serines/threonines to alanines are indicated in the five phosphoneprilysin mutants, S4A-, S6A-, T11A-, T15A-, and T25A-NEP. *B*, effects of NT-3 on the phosphorylation state of the intracellular domain of neprilysin. Primary neurons (*left*) were untreated or treated with NT-3 (100 ng/ml) or NT-3 together with U0126 for 24 h, as indicated, after which neprilysin was immunoprecipitated from 1 mg of cell lysate with neprilysin antibody, and the immunoprecipitates were analyzed by immunoblotting with phosphoneprilysin antibodies. Primary neurons expressing human neprilysin by infection with SFV-hNEP (*right*) were treated the same way as the non-infected primary neurons, as indicated. 150 μg of cell lysate was immunoprecipitated and immunoblotted with phosphoneprilysin antibodies, as indicated to the *right*. *N/A*, not applicable; *N.D*, not determined. *C*, densitometric quantification of Western blot data in *B*. Data represent the mean ± S.D. (*error bars*) ($n = 3$). *, $p < 0.05$, treated sample compared with non-treated or co-treated. *D*, cell surface-located proteins were biotinylated and pulled down using streptavidin beads, followed by immunoprecipitation (*IP*) of non-biotinylated neprilysin using a neprilysin antibody. Immunoprecipitates were subjected to Western blot analysis using the phosphoneprilysin antibodies pS4-NEP, pS6-NEP, pT11-NEP, pT15-NEP, pT25-NEP, and NEP (56C6). Western blot data of samples from two independent experiments are shown. At least three independent experiments were performed, and a similar band pattern was repeatedly verified. *E*, cell surface neprilysin activity of SH-SY5Y cells transiently expressing WT-, S4A-, S6A-, T11A-, T15A-, or T25A-NEP were evaluated using suc-Ala-Ala-Phe-MCA substrate. The neprilysin activities were normalized to neprilysin expression levels quantified by Western blot. Data represent the mean ± S.D. ($n = 3$). **, $p < 0.01$ compared with WT-NEP. *F*, SH-SY5Y cells transiently expressing WT-NEP or S6A-NEP were biotinylated, and the amount of biotinylated neprilysin was evaluated by a pull-down assay. Data represent the mean ± S.D. ($n = 3$). ***, $p < 0.01$ compared with WT-NEP. *G*, Aβ levels in the conditioned medium from SH-SY5Y cells transiently expressing WT-NEP or S6A-NEP. Data represent the mean ± S.D. ($n = 4$). **, $p < 0.01$ compared with WT-NEP. *H*, neprilysin activity in whole-cell lysates from WT-NEP and S6A-NEP transfectants was measured. Data represent the mean ± S.D. ($n = 3$). *I*, the effect of NT-3 on cell surface S6A-NEP activity. SH-SY5Y cells transiently expressing S6A-NEP were treated with NT-3 for 24 h. Cell surface neprilysin activity was measured using suc-Ala-Ala-Phe-MCA substrate. Data represent the mean ± S.D. ($n = 3$).

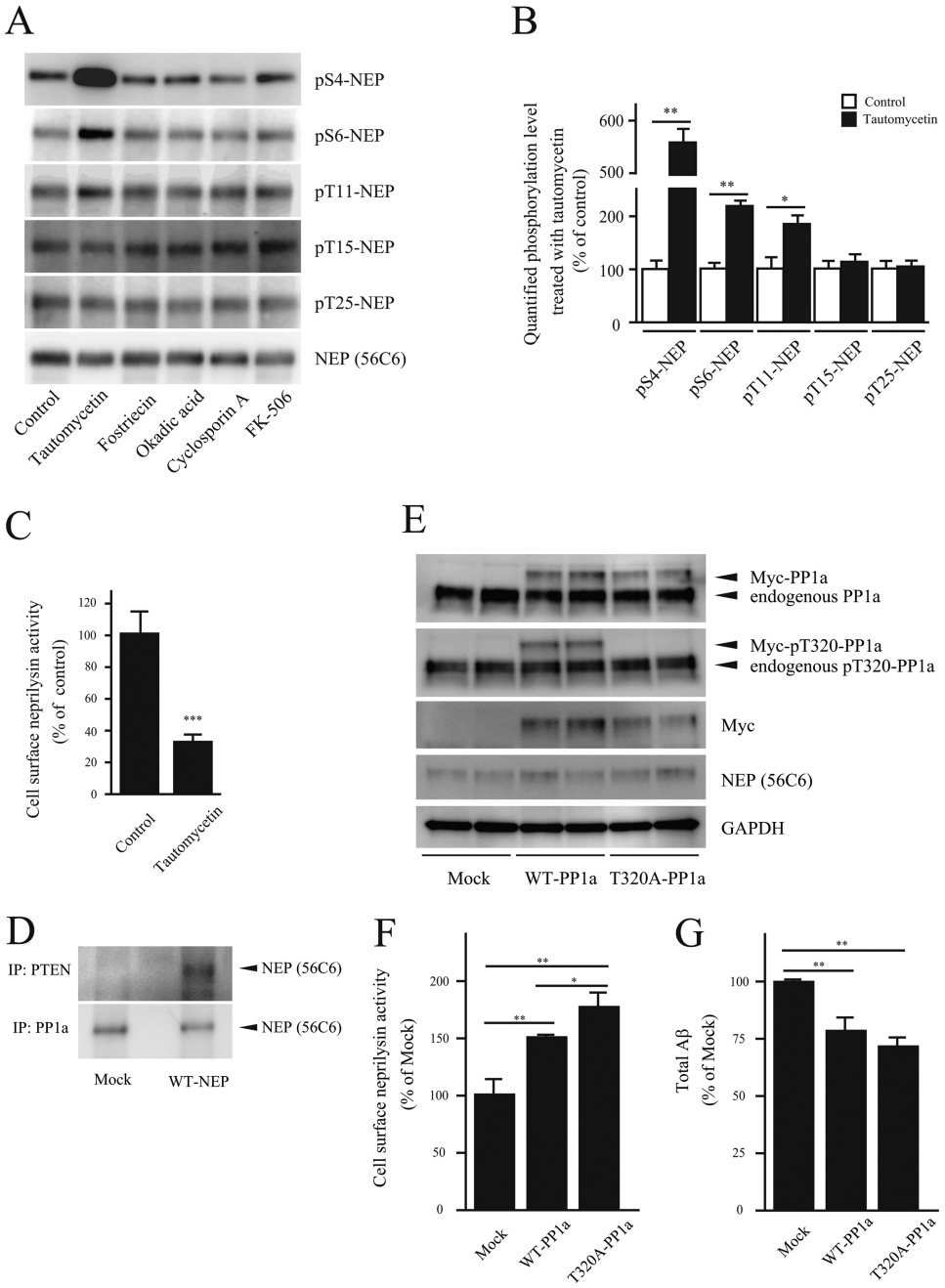

FIGURE 6. **PP1a regulates neprilysin activity through dephosphorylation.** *A*, primary neurons infected with SFV-hNEP were treated with specific inhibitors of serine/threonine phosphatases, tautomycetin (1 μM), fostriecin (100 nM), okadaic acid (10 nM), cyclosporin A (1 μM), and FK-506 (1 μM), and the phosphorylation state of neprilysin was measured by immunoprecipitation using a neprilysin antibody and immunoblot with phosphospecific antibodies. *B*, densitometric quantification of phosphorylation levels after tautomycetin treatment for 24 h as analyzed by Western blot in *A*. Data represent the mean ± S.D. (*error bars*) ($n = 3$). *, $p < 0.05$; **, $p < 0.01$ compared with non-treated. *C*, the effect of tautomycetin on cell surface neprilysin activity in primary neurons infected with SFV-hNEP. Data represent the mean ± S.D. ($n = 3$). **, $p < 0.01$ compared with control. *D*, immunoprecipitation (*IP*) of SH-SY5Y cell lysates with PTEN and PP1a antibodies. SH-SY5Y cells were transfected with a mock or WT-NEP expression vector. Lysates were prepared and immunoprecipitated using PTEN and PP1a antibodies as indicated. The immunoprecipitates were subjected to Western blot analysis, using anti-neprilysin antibody for detection. *E*, verification of WT- and T320A-PP1a expression in SH-SY5Y transfectants by Western blot and using antibodies as indicated to the *right*. *F*, the effect of PP1a activation on cell surface neprilysin activity. SH-SY5Y cells infected with SFV-hNEP were transfected with WT- or T320A-PP1a followed by measurement of cell surface neprilysin activity. Data represent the mean ± S.D. ($n = 4$). *, $p < 0.05$; **, $p < 0.01$ compared with control. *G*, effect of PP1a activation on Aβ levels. The Aβ levels in conditioned medium from WT- and T320A-PP1a-transfected SH-SY5Y cells, infected with SFV-hNEP, were quantified by ELISA. Data represent the mean ± S.D. ($n = 4$). **, $p < 0.01$ compared with control.

dence indicates the feasibility of a neprilysin-based approach. For example, overexpression of neprilysin leads to a decrease in Aβ load and improved memory in AD model mice. Another factor that argues in favor of a neprilysin-based treatment is the limited number of possible side effects. For example, the levels of neuropeptides in neprilysin knock-out mice are unaltered, indicating that proteases other than neprilysin are involved in their metabolism. Furthermore, neprilysin transgenic mice do not display other behavioral abnormalities (15–17, 39). However, in order to develop a neprilysin-based AD treatment, it is

essential to have a more detailed understanding of the mechanism of neprilysin activation and to identify a regulator of neprilysin activity.

In this report, we show that neurotrophic factors reduce cell surface neprilysin activity (Fig. 1 and supplemental Fig. S1) through regulation of cell surface neprilysin localization (Fig. 4) and that the reduction of neprilysin activity leads to increased Aβ levels (Fig. 3). On the other hand, previous extensive studies have shown that neurotrophic factors, particularly BDNF, exhibit neuroprotective properties that contribute to neuronal survival and memory formation in both rodent and primate models of AD through amyloid-independent mechanisms (40). In addition, BDNF also supports neural stem cells, which have been demonstrated to improve cognition in a transgenic model of AD (41). Furthermore, oligomeric Aβ has been shown to decrease cortical BDNF levels and synaptic function in an AD model mouse (42, 43). These findings together indicate that BDNF would be a useful adjunct in AD therapy to compensate for decreased levels of this neurotrophic factor in the brain and to ameliorate symptoms in the late stages of disease, whereas a strategy involving neprilysin activation could be effective in preventing or delaying the onset of AD because the facilitation of Aβ clearance would attenuate synaptic dysfunction and the reduction in BDNF levels. In fact, with accumulating knowledge, it appears that any treatment for AD is likely to be directed at several targets simultaneously. Our data show that a strategy involving any neurotrophic factor would have as a side effect increased Aβ levels that would have to be taken into account.

The use of neurotrophic factors in this study enabled us to unravel some of the mechanisms controlling neprilysin activity. We found that cell surface neprilysin activity is regulated through the localization of neprilysin to the cell surface, a process that in turn is mediated by phosphorylation/dephosphorylation of the NEP-ICD (Figs. 4 and 5). The regulation of neprilysin activity also involved MEK/ERK signaling, which resulted in phosphorylation of Ser-6 in the NEP-ICD (Figs. 2 and 5), although it remains unclear whether ERK directly phosphorylates the NEP-ICD. Interestingly, casein kinase 2 has been reported to act as a kinase for S6-NEP-ICD phosphorylation (44). Moreover, increased phosphorylation of neprilysin appeared after 24 h of stimulation, indicating that the expression of additional unknown factors might be required.

Although the mechanism remains unclear, metabolism of neprilysin itself would also influence its cell surface activity. Interestingly, T25A-NEP mutant protein could not be detected in transfected cells, despite the presence of the mRNA (supplemental Fig. S5). Speculatively, dephosphorylation of Thr-25 might induce degradation of neprilysin in the cells, as part of a quality control mechanism in the metabolic pathway of neprilysin, although Thr-25 was found to be dephosphorylated in neprilysin located at the cell surface (Fig. 5*D*). Alternatively, the introduced mutation could destabilize the protein and induce aggregation, although the S6A/T25A double mutant was normally expressed in the transfectants (data not shown).

The addition of the PP1a inhibitor tautomycetin to primary cortical/hippocampal neurons extensively increased the phosphorylation state of the NEP-ICD (Fig. 6, *A* and *B*) and reduced cell surface neprilysin activity (Fig. 6*C*). A closer examination of the NEP-ICD amino acid sequence revealed a peptide sequence, KKKQRW, similar to the PP1a binding motif, suggesting that the NEP-ICD might be a target of PP1a. Indeed, PP1a was found to be associated with neprilysin in SH-SY5Y cell extracts, and overexpression of PP1a stimulated cell surface neprilysin activity, leading to reduced Aβ levels (Fig. 6, *D–G*). Therefore, activation of PP1a (*e.g.* pharmacologically) would be a possible strategy to increase cell surface neprilysin activity. Interestingly, it has been reported that PP1a activity was regulated by DARPP32, an endogenous regulator of PP1a (45), and that DARPP32 levels are reduced in the brains of somatostatin receptor-1 (SSTR1) and SSTR5 double knock-out mice (46). These observations, considered together with our previous data showing that presynaptic localization of neprilysin is significantly decreased in the hippocampus of somatostatin-deficient mice (18), indicate that somatostatin possibly regulates neprilysin activity through PP1 activity. Thus, SSTR agonists might be successful drug candidates for the treatment of AD.

With the development of new gene therapy technologies, application of a neprilysin gene transfer strategy could be a potential way to decrease Aβ levels and delay the onset of amyloidosis. Considering the increased activity of S6-NEP, an alternative would be to introduce the S6A-NEP mutant, possibly leading to even more efficient Aβ degradation compared with that of WT-NEP.

In conclusion, our results show that the phosphorylation state of the intracellular domain regulates cell surface neprilysin activity and extracellular Aβ levels due to the modulation of neprilysin localization. We propose that enhancing cell surface neprilysin activity, for example by maintaining S6 of the NEP-ICD in a dephosphorylated state, either through activation of phosphatases or through inhibition of the kinase responsible for phosphorylation at the S6-NEP-ICD, would be beneficial for the prevention of Aβ amyloidosis.

Acknowledgment—We thank Dr. C. Gerard for providing neprilysin-deficient mice.

REFERENCES

1. Hardy, J., and Selkoe, D. J. (2002) The amyloid hypothesis of Alzheimer's disease. Progress and problems on the road to therapeutics. *Science* **297,** 353–356
2. Selkoe, D. J. (1994) Alzheimer's disease. A central role for amyloid. *J. Neuropathol. Exp. Neurol.* **53,** 438–447
3. Selkoe, D. J. (1994) Cell biology of the amyloid β-protein precursor and the mechanism of Alzheimer's disease. *Annu. Rev. Cell Biol.* **10,** 373–403
4. Saito, T., Suemoto, T., Brouwers, N., Sleegers, K., Funamoto, S., Mihira, N., Matsuba, Y., Yamada, K., Nilsson, P., Takano, J., Nishimura, M., Iwata, N., Van Broeckhoven, C., Ihara, Y., and Saido, T. C. (2011) Potent amyloidogenicity and pathogenicity of Aβ43. *Nat. Neurosci.* **14,** 1023–1032
5. Saido, T. C. (1998) Alzheimer's disease as proteolytic disorders. Anabolism and catabolism of β-amyloid. *Neurobiol. Aging* **19,** S69–S75
6. Iwata, N., Tsubuki, S., Takaki, Y., Shirotani, K., Lu, B., Gerard, N. P., Gerard, C., Hama, E., Lee, H. J., and Saido, T. C. (2001) Metabolic regulation of brain Aβ by neprilysin. *Science* **292,** 1550–1552
7. Iwata, N., Tsubuki, S., Takaki, Y., Watanabe, K., Sekiguchi, M., Hosoki, E., Kawashima-Morishima, M., Lee, H. J., Hama, E., Sekine-Aizawa, Y., and Saido, T. C. (2000) Identification of the major Aβ1–42-degrading catabolic pathway in brain parenchyma. suppression leads to biochemical and pathological deposition. *Nat. Med.* **6,** 143–150

8. Caccamo, A., Oddo, S., Sugarman, M. C., Akbari, Y., and LaFerla, F. M. (2005) Age- and region-dependent alterations in Aβ-degrading enzymes. implications for Aβ-induced disorders. *Neurobiol. Aging* **26,** 645–654
9. Reilly, C. E. (2001) Neprilysin content is reduced in Alzheimer brain areas. *J. Neurol.* **248,** 159–160
10. Carter, T. L., Pedrini, S., Ghiso, J., Ehrlich, M. E., and Gandy, S. (2006) Brain neprilysin activity and susceptibility to transgene-induced Alzheimer amyloidosis. *Neurosci. Lett.* **392,** 235–239
11. Iwata, N., Takaki, Y., Fukami, S., Tsubuki, S., and Saido, T. C. (2002) Region-specific reduction of Aβ-degrading endopeptidase, neprilysin, in mouse hippocampus upon aging. *J. Neurosci. Res.* **70,** 493–500
12. Yasojima, K., Akiyama, H., McGeer, E. G., and McGeer, P. L. (2001) Reduced neprilysin in high plaque areas of Alzheimer brain. A possible relationship to deficient degradation of β-amyloid peptide. *Neurosci. Lett.* **297,** 97–100
13. Huang, S. M., Mouri, A., Kokubo, H., Nakajima, R., Suemoto, T., Higuchi, M., Staufenbiel, M., Noda, Y., Yamaguchi, H., Nabeshima, T., Saido, T. C., and Iwata, N. (2006) Neprilysin-sensitive synapse-associated amyloid-β peptide oligomers impair neuronal plasticity and cognitive function. *J. Biol. Chem.* **281,** 17941–17951
14. Farris, W., Schütz, S. G., Cirrito, J. R., Shankar, G. M., Sun, X., George, A., Leissring, M. A., Walsh, D. M., Qiu, W. Q., Holtzman, D. M., and Selkoe, D. J. (2007) Loss of neprilysin function promotes amyloid plaque formation and causes cerebral amyloid angiopathy. *Am. J. Pathol.* **171,** 241–251
15. Iwata, N., Mizukami, H., Shirotani, K., Takaki, Y., Muramatsu, S., Lu, B., Gerard, N. P., Gerard, C., Ozawa, K., and Saido, T. C. (2004) Presynaptic localization of neprilysin contributes to efficient clearance of amyloid-β peptide in mouse brain. *J. Neurosci.* **24,** 991–998
16. El-Amouri, S. S., Zhu, H., Yu, J., Marr, R., Verma, I. M., and Kindy, M. S. (2008) Neprilysin. An enzyme candidate to slow the progression of Alzheimer's disease. *Am. J. Pathol.* **172,** 1342–1354
17. Leissring, M. A., Farris, W., Chang, A. Y., Walsh, D. M., Wu, X., Sun, X., Frosch, M. P., and Selkoe, D. J. (2003) Enhanced proteolysis of β-amyloid in APP transgenic mice prevents plaque formation, secondary pathology, and premature death. *Neuron* **40,** 1087–1093
18. Saito, T., Iwata, N., Tsubuki, S., Takaki, Y., Takano, J., Huang, S. M., Suemoto, T., Higuchi, M., and Saido, T. C. (2005) Somatostatin regulates brain amyloid β peptide Aβ42 through modulation of proteolytic degradation. *Nat. Med.* **11,** 434–439
19. Saido, T. C., Nagao, S., Shiramine, M., Tsukaguchi, M., Sorimachi, H., Murofushi, H., Tsuchiya, T., Ito, H., and Suzuki, K. (1992) Autolytic transition of μ-calpain upon activation as resolved by antibodies distinguishing between the pre- and post-autolysis forms. *J. Biochem.* **111,** 81–86
20. Saido, T. C., Iwatsubo, T., Mann, D. M., Shimada, H., Ihara, Y., and Kawashima, S. (1995) Dominant and differential deposition of distinct beta-amyloid peptide species, Aβ N3(pE), in senile plaques. *Neuron* **14,** 457–466
21. Pagans, S., Sakane, N., Schnölzer, M., and Ott, M. (2011) Characterization of HIV Tat modifications using novel methyl-lysine-specific antibodies. *Methods* **53,** 91–96
22. Hussain, I., Hawkins, J., Harrison, D., Hille, C., Wayne, G., Cutler, L., Buck, T., Walter, D., Demont, E., Howes, C., Naylor, A., Jeffrey, P., Gonzalez, M. I., Dingwall, C., Michel, A., Redshaw, S., and Davis, J. B. (2007) Oral administration of a potent and selective non-peptidic BACE-1 inhibitor decreases β-cleavage of amyloid precursor protein and amyloid-β production *in vivo*. *J. Neurochem.* **100,** 802–809
23. Shirotani, K., Tsubuki, S., Iwata, N., Takaki, Y., Harigaya, W., Maruyama, K., Kiryu-Seo, S., Kiyama, H., Iwata, H., Tomita, T., Iwatsubo, T., and Saido, T. C. (2001) Neprilysin degrades both amyloid β peptides 1–40 and 1–42 most rapidly and efficiently among thiorphan- and phosphoramidon-sensitive endopeptidases. *J. Biol. Chem.* **276,** 21895–21901
24. Berndt, N., Dohadwala, M., and Liu, C. W. (1997) Constitutively active protein phosphatase 1α causes Rb-dependent G_1 arrest in human cancer cells. *Curr. Biol.* **7,** 375–386
25. Hama, E., Shirotani, K., Iwata, N., and Saido, T. C. (2004) Effects of neprilysin chimeric proteins targeted to subcellular compartments on amyloid β peptide clearance in primary neurons. *J. Biol. Chem.* **279,** 30259–30264
26. Takaki, Y., Iwata, N., Tsubuki, S., Taniguchi, S., Toyoshima, S., Lu, B., Gerard, N. P., Gerard, C., Lee, H. J., Shirotani, K., and Saido, T. C. (2000) Biochemical identification of the neutral endopeptidase family member responsible for the catabolism of amyloid β peptide in the brain. *J. Biochem.* **128,** 897–902
27. Rappoport, J. Z., and Simon, S. M. (2003) Real-time analysis of clathrin-mediated endocytosis during cell migration. *J. Cell Sci.* **116,** 847–855
28. Barbacid, M. (1994) The Trk family of neurotrophin receptors. *J. Neurobiol.* **25,** 1386–1403
29. Segal, R. A., and Greenberg, M. E. (1996) Intracellular signaling pathways activated by neurotrophic factors. *Annu. Rev. Neurosci.* **19,** 463–489
30. Segal, R. A. (2003) Selectivity in neurotrophin signaling. Theme and variations. *Annu. Rev. Neurosci.* **26,** 299–330
31. Loeb, D. M., Tsao, H., Cobb, M. H., and Greene, L. A. (1992) NGF and other growth factors induce an association between ERK1 and the NGF receptor, gp140prototrk. *Neuron* **9,** 1053–1065
32. Zheng, H., and Koo, E. H. (2006) The amyloid precursor protein. Beyond amyloid. *Mol. Neurodegener.* **1,** 5
33. Eckman, E. A., Watson, M., Marlow, L., Sambamurti, K., and Eckman, C. B. (2003) Alzheimer's disease β-amyloid peptide is increased in mice deficient in endothelin-converting enzyme. *J. Biol. Chem.* **278,** 2081–2084
34. Farris, W., Mansourian, S., Chang, Y., Lindsley, L., Eckman, E. A., Frosch, M. P., Eckman, C. B., Tanzi, R. E., Selkoe, D. J., and Guenette, S. (2003) Insulin-degrading enzyme regulates the levels of insulin, amyloid β-protein, and the β-amyloid precursor protein intracellular domain *in vivo*. *Proc. Natl. Acad. Sci. U.S.A.* **100,** 4162–4167
35. Pawson, T., and Scott, J. D. (1997) Signaling through scaffold, anchoring, and adaptor proteins. *Science* **278,** 2075–2080
36. Sumitomo, M., Iwase, A., Zheng, R., Navarro, D., Kaminetzky, D., Shen, R., Georgescu, M. M., and Nanus, D. M. (2004) Synergy in tumor suppression by direct interaction of neutral endopeptidase with PTEN. *Cancer Cell* **5,** 67–78
37. Roy, J., and Cyert, M. S. (2009) Cracking the phosphatase code. Docking interactions determine substrate specificity. *Sci. Signal.* **2,** re9
38. Hurley, T. D., Yang, J., Zhang, L., Goodwin, K. D., Zou, Q., Cortese, M., Dunker, A. K., and DePaoli-Roach, A. A. (2007) Structural basis for regulation of protein phosphatase 1 by inhibitor-2. *J. Biol. Chem.* **282,** 28874–28883
39. Iwata, N., Higuchi, M., and Saido, T. C. (2005) Metabolism of amyloid-beta peptide and Alzheimer's disease. *Pharmacol. Ther.* **108,** 129–148
40. Nagahara, A. H., Merrill, D. A., Coppola, G., Tsukada, S., Schroeder, B. E., Shaked, G. M., Wang, L., Blesch, A., Kim, A., Conner, J. M., Rockenstein, E., Chao, M. V., Koo, E. H., Geschwind, D., Masliah, E., Chiba, A. A., and Tuszynski, M. H. (2009) Neuroprotective effects of brain-derived neurotrophic factor in rodent and primate models of Alzheimer's disease. *Nat. Med.* **15,** 331–337
41. Blurton-Jones, M., Kitazawa, M., Martinez-Coria, H., Castello, N. A., Müller, F. J., Loring, J. F., Yamasaki, T. R., Poon, W. W., Green, K. N., and LaFerla, F. M. (2009) Neural stem cells improve cognition via BDNF in a transgenic model of Alzheimer disease. *Proc. Natl. Acad. Sci. U.S.A.* **106,** 13594–13599
42. Peng, S., Garzon, D. J., Marchese, M., Klein, W., Ginsberg, S. D., Francis, B. M., Mount, H. T., Mufson, E. J., Salehi, A., and Fahnestock, M. (2009) Decreased brain-derived neurotrophic factor depends on amyloid aggregation state in transgenic mouse models of Alzheimer's disease. *J. Neurosci.* **29,** 9321–9329
43. Zheng, Z., Sabirzhanov, B., and Keifer, J. (2010) Oligomeric amyloid-β inhibits the proteolytic conversion of brain-derived neurotrophic factor (BDNF), AMPA receptor trafficking, and classical conditioning. *J. Biol. Chem.* **285,** 34708–34717
44. Siepmann, M., Kumar, S., Mayer, G., and Walter, J. (2010) Casein kinase 2 dependent phosphorylation of neprilysin regulates receptor tyrosine kinase signaling to Akt. *PLoS One* **5,** e13134
45. Greengard, P., Allen, P. B., and Nairn, A. C. (1999) Beyond the dopamine receptor. The DARPP-32/protein phosphatase-1 cascade. *Neuron* **23,** 435–447
46. Rajput, P. S., Kharmate, G., Norman, M., Liu, S. H., Sastry, B. R., Brunicardi, C. F., and Kumar, U. (2011) Somatostatin receptor 1 and 5 double knockout mice mimic neurochemical changes of Huntington's disease transgenic mice. *PLoS One* **6,** e24467